

## **Middle School Rain and Falling Snow Measurements**

Shelby Fuller (University of Wyoming) and Jefferson Snider (University of Wyoming)

**Abstract:** This outreach program started with an email from a colleague who was offering two automatic precipitation gauges. The gauges originated from a well-known vendor and were only a few years old. We accepted the offer, configured the gauges to communicate with a computer, developed analysis and display software, and inquired in the Laramie K-12 community to see if there was interest in collaboration. The Laramie Middle School accepted. Four years on, the collaboration has addressed the following topics: (1) the atmospheric side of the water cycle (i.e., rain and falling snow), (2) the development of a meteorology curriculum at Laramie Middle School, (3) student involvement in the precipitation measurements, (4) display of measurements, and (5) analysis of precipitation and temperature data recorded at the middle school. We have also consulted the Next Generation Science Standards for weather and climate curricula in US middle schools and aligned this outreach program to those recommendations. Finally, we show how our analysis of data from the Middle School conforms with findings of professional meteorologists using state-of-the-art instrumentation deployed at numerous sites across the globe.

## INTRODUCTION

Precipitation is a vital element of the Earth system. Where it is forecast to occur affects the planning of individuals, communities, regions, and nations. For these reasons, there is a clear justification for measuring precipitation. From a scientific perspective, the measurement of precipitation is important for understanding Earth's atmospheric, hydrological, and energy cycles. Improved weather forecasts, and improved weather notification, are two societal benefits that stem from making and analyzing precipitation measurements.

Our outreach program explains precipitation measurements to 6<sup>th</sup> and 7<sup>th</sup> graders at Laramie Middle School (LMS). We do this by engaging with one of the measurement systems used by meteorologists: the automatic weighing precipitation gauge. In addition to describing the "why" of gauge-based precipitation measurement, we describe the "how." The main concept is that gauges measure the mass of precipitation that falls through a horizontal area in a unit of time. We show how this mass flux is converted to a depth of liquid water appearing at the surface in the same unit of time (precipitation rate). Further, we explain that this transformation involves a material property, density, and that, by convention, it is the density of liquid water (1 gram per cubic centimeter) that is applied in the conversion. The conversion is done regardless of precipitation type (rain or falling snow), and in the case of falling snow, the resultant is called the liquid-equivalent precipitation rate. For snowfall, we also show how a precipitation rate is used to calculate the rate of snow depth increase. Commonly, the factor used to estimate the rate of snow depth increase is ten-to-one. But in Wyoming, where falling snow is unusually fluffy, the multiplier can be as large as twenty-to-one. Clearly, if the snow melts as it reaches the surface, or if the snow is drifted by wind, weighing-gauge estimates of either snow depth or of the rate of snow depth increase are incorrect.

Results presented here come from analyses of gauge measurements recorded at the LMS. We present diurnal and annual cycles of temperature and precipitation, similarities and differences among warm season (rain) and cold season (falling snow) precipitation events, a comparison of sheltered- and exposed-gauge measurements, and a statistical analysis of precipitation rate and temperature. Our findings are summarized in the Conclusion.

## MEASUREMENTS

Measurements from two Vaisala All Weather Precipitation Gauges (VRG; Vaisala 2007) are recorded at the LMS. The gauges record the mass of the collecting container, the temperature of the VRGs' electronics enclosure, and the liquid-equivalent precipitation rate. A statistical comparison of measurements from the National Weather Service and from the VRGs, is the basis for our conversion of enclosure temperature to ambient temperature. Recordings from both gauges are transmitted to a custom-built data interface. The latter decodes and transmits via Ethernet to a personal computer where the data is recorded. The computer records measurements from the two gauges in separate ASCII files. The interval between measurements is one minute, thus the sampling frequency is  $1 \text{ min}^{-1}$ . Measurement accuracies are  $\pm 2 \text{ g}$ ,  $\pm 0.1 \text{ mm/hr}$ ,  $\pm 2 \text{ }^\circ\text{C}$ , and  $\pm 0.01 \text{ min}^{-1}$  for mass, precipitation rate, ambient temperature, and sample frequency, respectively. The VRGs are installed at different locations near the LMS. A sheltered gauge is installed in a garden area. South-facing and west-facing walls of the LMS define two sides of the garden. An exposed gauge is  $\sim 10 \text{ m}$  south of the LMS. Both gauges are within 5 m of spruce

trees and the trees are ~ 10 m tall. The gauge openings are 2 m above ground level. The exposed and sheltered gauges are shown in Fig. 1a – b.

The computer code that drives real-time presentation of the gauge data is provided online<sup>1</sup>. Results are output to a hallway display at the LMS. The data display is started at 7 AM and ended at 4 PM.

## DATA AND RELEVANCE TO THE SCIENCE STANDARDS

The figures 2a – b and 3a – b are presented to highlight some of the patterns evident in the temperature and precipitation data collected at the LMS. We are using these data products to engage students in ways recommended for K-12 science education by the National Research Council (NRC, 2012; Next Generation Science Standards 2014). There are three dimensions to this. First, figures 2a and 3a connect to the notion that “warmth”, expressed by temperature, is larger during summer. We emphasize, in our presentation to the LMS students, that this is an example of why practitioners *carryout measurements* and how this information can be used to strengthen understanding of seasonal and climate variability. Second, Fig. 2b shows that precipitation rates are generally larger during the summer. Moreover, since the y axis in this figure is logarithmic, the summertime enhancement of precipitation rate is quite significant. Thus, figures 2b and 3b relate to a core idea in the NRC recommendations; specifically *the role of the water cycle in Earth processes*. Finally, a key concept underlying all of the results shown in figures 2a – b and 3a – b is that a signal, coming from an electronic sensor, is input to a calculation, and that the output of the calculation is the temperature (or precipitation) value that is graphed. This is an example of a crosscutting concept emphasized by the NRC, specifically the *importance of measurement in gaining insight into how systems operate*. Fig. 3a – b, with its focus on one month (July 2018), further exemplifies the primacy of measurement and the insight it can provide. Evident here is a pronounced night-to-day variation of temperature and the absence of temperature variation due to the passage of weather systems which, during winter months (e.g., during February in Fig. 2a), drive temperatures at least ten degrees colder than the climatological average. In addition, several short-duration intervals with precipitation rates in excess of 10 mm/hr are seen in Fig. 3b. These features are characteristic of summertime rain showers.

## PRECIPITATION RELATIONSHIPS

Many relationships are used to quantify precipitation. One of these has been called, euphemistically, the First Law of Precipitation (attributable to C.F. Chappell). This relates a storm-total precipitation amount ( $P$ ; expressed as a liquid-equivalent depth), the duration of a precipitation event ( $D$ ), and an effective precipitation rate ( $R$ ):

$$P = D \times R \quad (1)$$

Two precipitation events recorded at the LMS are shown in Fig. 4a – b. The first example (Fig. 4a) is falling snow (temperature  $\leq 0$  °C) and the second (Fig. 4b) is rain (temperature  $\geq 5$  °C).

---

<sup>1</sup> [http://www-das.uwyo.edu/~jsnider/firstPass\\_v3.py](http://www-das.uwyo.edu/~jsnider/firstPass_v3.py)

The precipitation amounts are 5 and 4 mm, respectively (data not shown). Consistent with Eq. 1, we can see that the longer duration of the snow event compensates for its generally smaller precipitation rate, making the amount of precipitation documented for the snow event (5 mm) larger than that during the rain event (4 mm). These examples also demonstrate that the effective rate, mentioned above, is an abstraction. In spite of this, the practical utility of Eq. 1 is that it connects two attributes of a precipitation event (rate and duration) to the attribute with the greatest societal impact (amount). It is also worth emphasizing that gauge measurements of all three attributes (amount, rate, and duration) are used retrospectively to improve forecast models and forecaster skill.

## **GAUGE COMPARISON**

Because we have two gauges at the LMS, it is logical to compare precipitation measurements from these two systems. The following comparison is based on 36 precipitation events (rain and falling snow) recorded between November 2017 and March 2019. We have restricted the comparison to events with amount  $> 1$  mm. Measurements from the sheltered gauge are plotted versus those from the exposed gauge in Fig. 5a – b. Since we have verified that measurements from the two gauges are calibrated to within  $\pm 2$  g (see Measurements Section), and since we cannot rationalize why atmospheric precipitation would vary systematically over the distance between the gauges, we conjecture that the difference seen in Fig. 5 (sheltered  $>$  exposed) is attributable to the different surroundings of the gauges (cf. Fig. 1a – b). One aspect of this is the smaller wind speed expected for the sheltered gauge. We expect this to create steeper precipitation particle trajectories (i.e., at the gauge opening), and thus a larger particle catch efficiency at the sheltered gauge. The other side of this is that the sheltered gauge may catch drifted particles (blowing snow), leading to inadvertent catch of snow particles that have re-entered the air stream after falling to the roof of the LMS. These issues complicate accurate monitoring of falling snow by professional meteorologists (Goodison et al. 1998).

## **CONNECTION TO GLOBAL WARMING**

In the previous section, and in Fig. 5a – b, we presented data from 36 precipitation events recorded at the LMS. We now investigate the degree of correlation between peak precipitation rates (henceforth peak rates) and coincident temperatures. Specifically, we want to see if the relation between peak rate and temperature, at the LMS, resembles that reported by professional meteorologists (e.g., Panthou et al 2014). Implications of this correlation, in investigations of global warming, are discussed in the conclusion.

Example peak rates for two precipitation events are shown in Fig. 4a – b. These figures only show peak rates evaluated by the sheltered gauge. We have also analyzed peak rates evaluated by the exposed gauge, but for brevity we only present results based on the sheltered gauge measurements.

Fig. 6a shows the frequency of occurrence of peak rates. In rough terms, the two modes evident in the histogram correspond to precipitation events that occurred during the cold seasons (i.e., Fall, Winter, and Spring) and during the warm season (Summer). In Fig. 6b, bin-averaged peak rates are plotted as a function of bin-midpoint temperature. Following Panthou et al (2014), we

calculated values of the logarithm of the averaged peak rate, correlated those with bin-midpoint temperatures using linear least-squares regression, and derived the dashed line in Fig. 6c. Statistics written above Fig. 6c demonstrate that there is a significant positive correlation between peak rate and temperature ( $p < 0.01$ ). Interpreted physically, the slope of the regression indicates that peak rate increases at  $8.7 \% \text{ } ^\circ\text{C}^{-1}$ . In addition, Fig. 6c shows that uncertainty associated with the slope of the dashed line is quite large ( $3.4 \% \text{ } ^\circ\text{C}^{-1}$ ). Based on these results, we can say that our slope differs *insignificantly* from either an analysis based on the Clausius-Clapeyron equation ( $\sim 6$  to  $7 \% \text{ } ^\circ\text{C}^{-1}$ ; Schneider et al. 2010) or based on sub-daily gauge data collected between May and October in southern Canada ( $\sim 7 \% \text{ } ^\circ\text{C}^{-1}$ ; Panthou et al 2014).

Fig. 7 presents a conceptual model of two processes that may contribute to the temperature-dependence of precipitation rate. At cloud base, vapor amount is larger in a warmer setting. The mass of vapor at cloud base (e.g., in a unit volume of air) increases at 6 to  $7 \% \text{ } ^\circ\text{C}^{-1}$  (i.e., at the rate predicted by the Clausius-Clapeyron equation; Schneider et al. 2010). Within a cloud updraft, water vapor apportions to cloud condensate. The temperature dependence of this apportionment is smaller than predicted by the Clausius-Clapeyron equation, but it is substantial ( $\sim 4$  to  $5 \% \text{ } ^\circ\text{C}^{-1}$ ; Albrecht et al. 1990). In real clouds, a plethora of processes, both macroscopic and microscopic, complicate the purely thermodynamic view presented in Fig. 7.

## CONCLUSION

Throughout this presentation we have sidelined discussion of how the LMS curriculum has changed as a result of our interaction with the LMS faculty. Even though we have participated in the development, the bulk of that effort has been the work of Joel Kropf, Dan Bremer, and Kim Burkhart. Rather, we view our involvement as professional role models, trained in the collection and analysis of meteorological data, and hopefully effective at explaining precipitation measurement to 6<sup>th</sup> and 7<sup>th</sup> graders. We have presented at the LMS in 2017, 2018, and 2019; this outreach amounts to 200 student contact hours per year.

Our primary emphasis has been on data collection, real-time display of measurements, data analysis, and how these activities connect to pedagogical recommendations of the National Research Council (NRC, 2012). What we have described also extends beyond pedagogy. Significantly, we have *rediscovered* two compelling aspects of precipitation science. The first deals with measurement of wind-driven falling snow and rain. We find that precipitation amounts derived using a sheltered gauge are consistently larger than those using an exposed gauge. Because we do not have wind measurements to augment this finding, and because of the possible confounding effect of blowing snow collected by the sheltered gauge, we cannot explore this in greater detail. The second involves a statistical link between measurements of peak precipitation rate and temperature. As in the previous case, we cannot claim this as a discovery. Rather, we have emphasized that our finding, when paired with results from data sets many times larger, can help society as it prepares for enhancements of the water cycle in the face of global warming. Finally, these rediscoveries, put in perspective, actually represent limitations in current understanding of weather and climate. As such, the broad intent of this outreach activity is its motivation of future scientists and engineers, so that they can participate in improving understanding of Earth's water cycle.

## **ACKNOWLEDGEMENTS**

We acknowledge support from Engineering's Next Generation Program established by the Ellbogen Foundation, the University of Wyoming College of Engineering and Applied Science, and the Wyoming Water Development Commission. We also acknowledge assistance from Matt Burkhart, Ben Heesen, Joel Kropf, Dan Bremer, Kim Burkhart, Nick Zelasko, and Noah Snider.

## **BIBLIOGRAPHY**

Albrecht, B.A., C.W.Fairall, D.W.Thomson and A.B.White, Surface-based remote sensing of the observed and the adiabatic liquid water content of stratocumulus clouds, *Geophys. Res. Lett.*, 17, 89-92, 1990

Goodison, B. E., Louie, P. Y. T., and Yang, D., WMO solid precipitation measurement intercomparison, WMO Tech. Doc. 872, 211 pp., 1998

National Research Council, A Framework for K-12 Science Education: Practices, Crosscutting Concepts, and Core Ideas. Washington, DC: The National Academies Press.  
<https://doi.org/10.17226/13165>, 2012

Next Generation Science Standards, accessed 26 March 2018 at:  
<https://www.nextgenscience.org/topic-arrangement/msweather-and-climate>, 2014

Panthou, G., A. Mailhot, E. Laurence, and G. Talbot, Relationship between Surface Temperature and Extreme Rainfalls: A Multi-Time-Scale and Event-Based Analysis, *J. Hydrometeor.*, 15, 1999–2011, <https://doi.org/10.1175/JHM-D-14-0020.1>, 2014

Schneider, T., O'Gorman, P. A., and Levine, X. J., Water vapor and the dynamics of climate changes, *Rev. Geophys.*, 48, RG3001, doi:10.1029/2009RG000302, 2010

Vaisala, Users Guide, Vaisala All Weather Precipitation Gauge, Vaisala, Inc., 67 pp., 2007



Figure 1: **Top)** Exposed gauge at the LMS. Older gauges, replaced during this outreach program, are seen against a south-facing wall of the school. **Bottom)** Sheltered gauge in the garden area near the south entrance to the LMS.

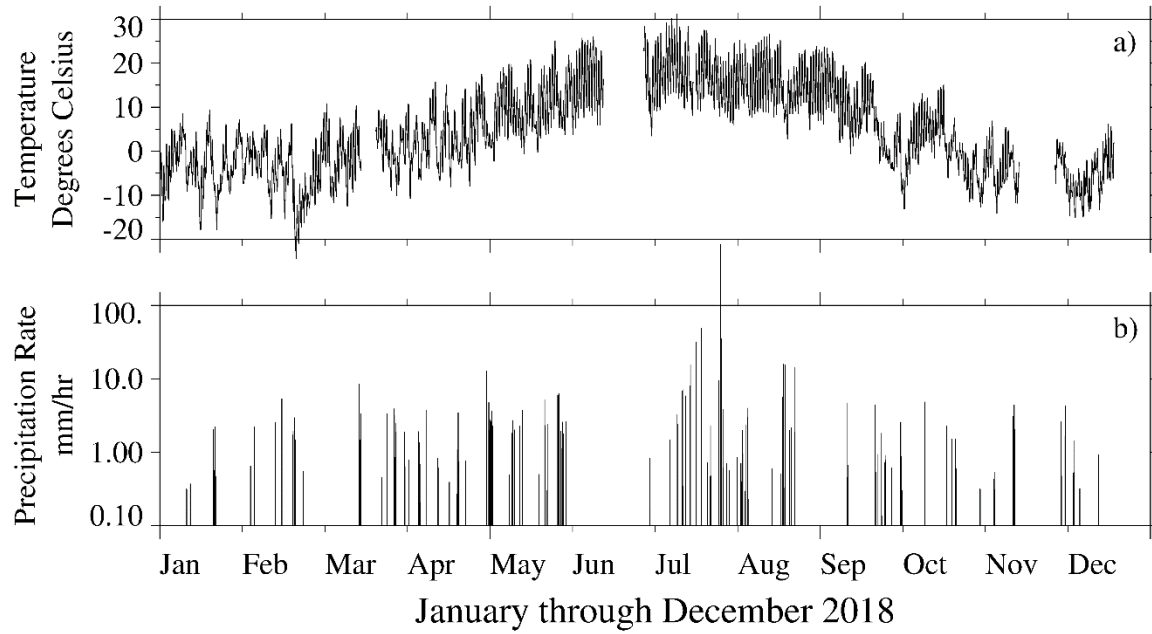


Figure 2: Measurements from the sheltered gauge. **a)** Temperature during 2018. **b)** Precipitation rate during 2018. Note the logarithmic y axis.

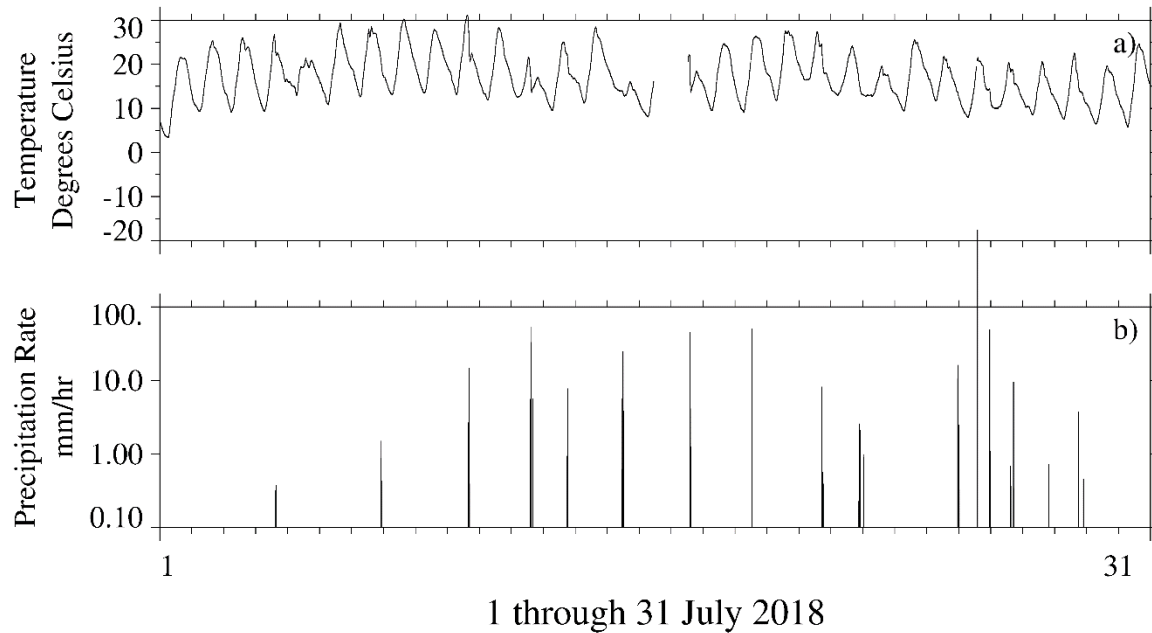


Figure 3: Measurements from the sheltered gauge. **a)** Temperature during July 2018. **b)** Precipitation rate during July 2018. Note the logarithmic y axis.

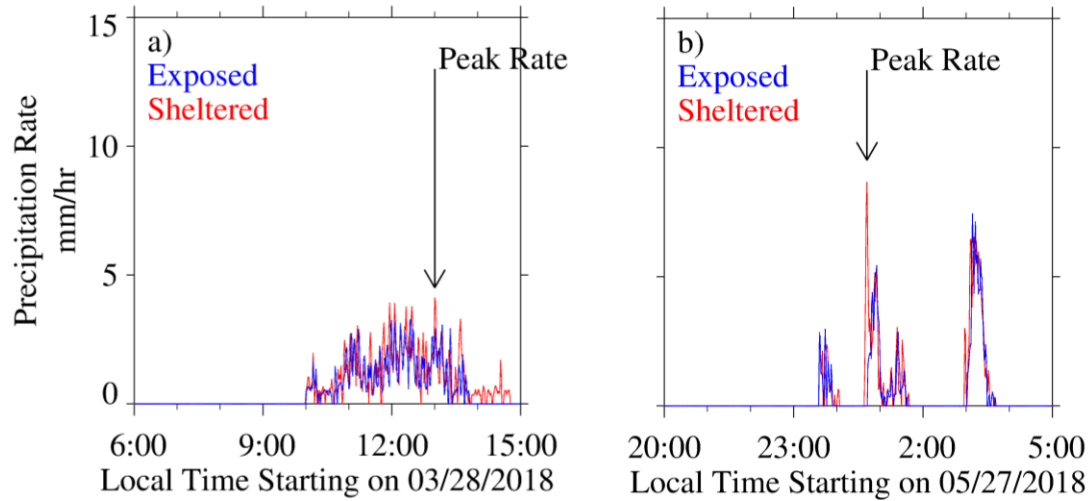


Figure 4: Precipitation events recorded at the LMS. **a)** Falling snow event with temperature  $\leq 0$  °C. **b)** Rain event with temperature  $\geq 5$  °C.

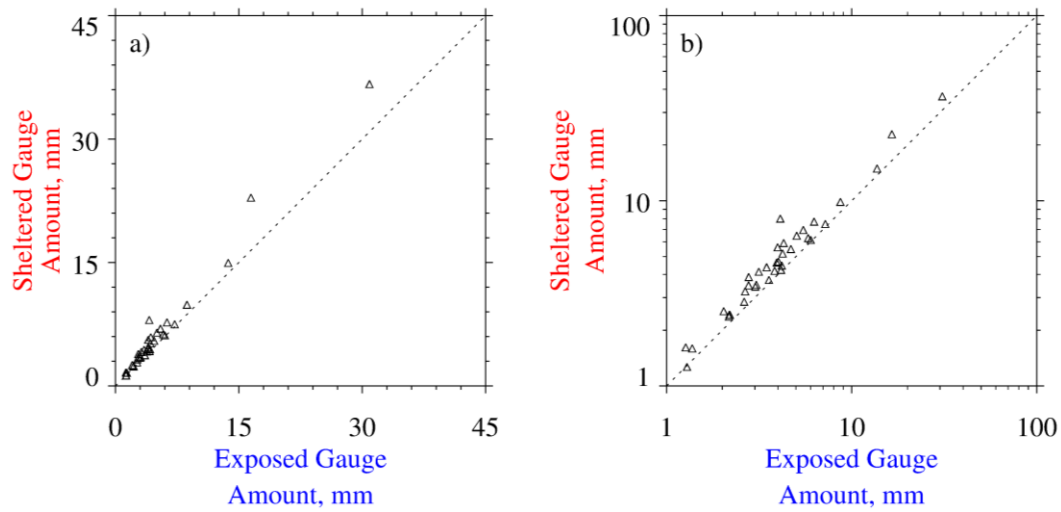


Figure 5: Comparison of precipitation amounts measured made at LMS. **a)** Comparison on linear axes. **b)** Comparison on logarithmic axes.

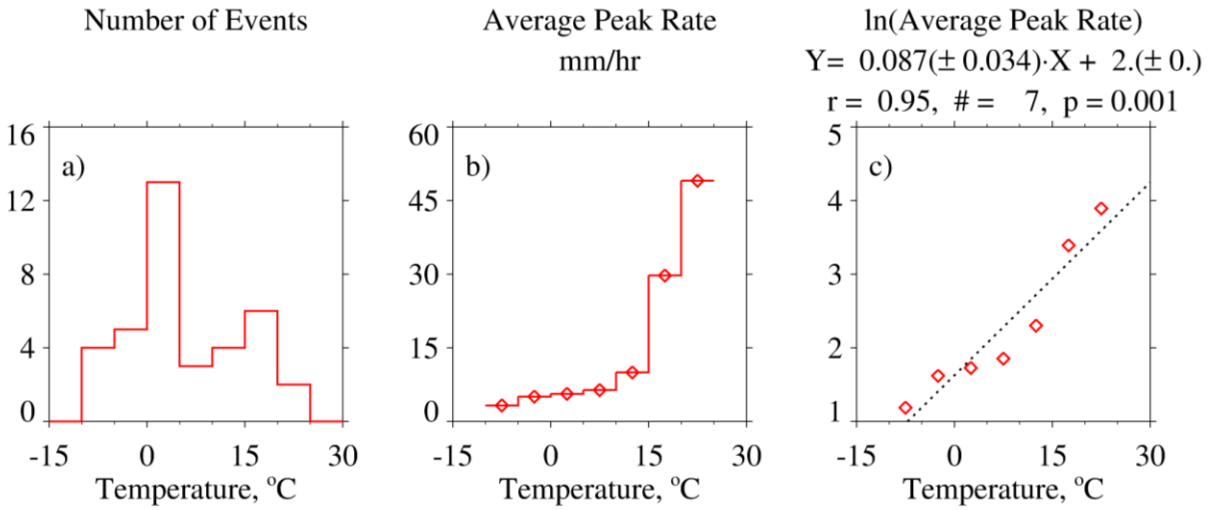


Figure 6: **a)** Frequency histogram of precipitation events binned by temperature. **b)** Bin-averaged peak precipitation rates vs bin-midpoint temperature. **c)** Scatterplot of the logarithm of the averaged peak rate vs bin-midpoint temperature.

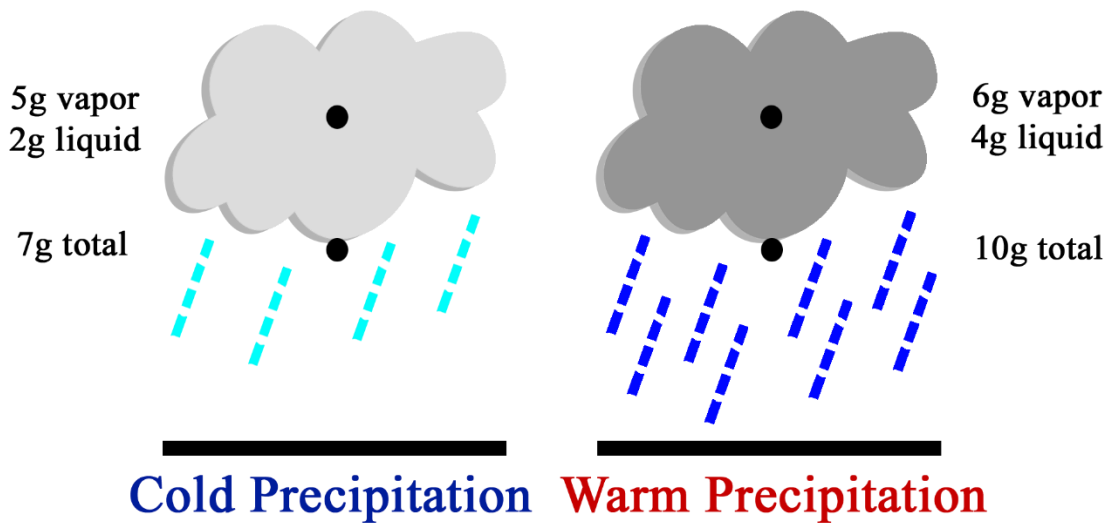


Figure 7: Thermodynamic controls on precipitation from two storms with differing cloud base temperature. The estimates of in-cloud vapor and liquid mass assume that air ascends in closed parcels from cloud base to inside the cloud.